
Production of Digital Elevation Model of Marvdasht Plain Using ENVISATASAR Radar Images with C-Wavelength Comparison with GPS Points and 1:25000 Topographic Maps of South Zagros Region

Alireza Karimi^{a*}

^a*Master's of Remote Sensing and GIS, Yazd Branch, Islamic Azad University, Yazd, Iran*

Received 09 February 2021; Revised 09 April 2021; Accepted 07 June 2021

Abstract

Digital Elevation Model is a continuous statistical representation of the earth by a large number of selected points with known coordinates of length, width and height. The use of three-dimensional models of the earth's surface has a wide range of applications in many areas of research and implementation. It is high and the areas are level. All the resulting points have a height above sea level. Most GIS spatial analyzes use elevation data such as DEM. Using it, you can prepare a slope map and slope direction and perform various analyzes in three dimensions. Most of the time, DEM is also used as the bottom view of the maps. Elevation is used to extract height and height data. Major users (DEM) in the fields of civil engineering, surveying and photogrammetry, earth sciences, water resources management, military applications, telecommunications, urban planning digital land models as one of their information layers to achieve management, executive goals or produce new products using location-based. In this study, using images of ASAR ENVI SAT sensors in C band in the study area, we prepared a digital elevation model and then compared. And for verification, we compared this prepared model with the existing topographic maps at the scale of 1:25000 as well as the fixed points of GPS stations and also with the digital model obtained from (SRTM) in terms of elevation. The results of radar image processing in C bands of ENVI SAT ASAR sensor and its comparison with the data of the surveying organization indicate that the data processed from C band gives more favorable results and close to the ground control points, but considering Due to the correlation between GCP points and DEM obtained from topography, production conditions using satellite images are not favorable for the region. GCP captured the height points of radar images are in better and more favorable conditions according to Table (4) which shows the standard difference and this indicates the superiority of radar images for DEM production. Digital model comparison ratio with topographic points, shows the accuracy of satellite images in flat areas. In mountainous areas, due to the inclination of the points and creation of incoherence points, it is not continuous shadow and the level curve lines are intermittent.

Keywords: Digital DEM Altitude Model, Interference Measurement, GCP & GPS Points, C Band, Sensor ASAR

* Corresponding author Tel: +98-9301136836.
Email address: arkarimi0455@gmail.com.

1. Introduction

Digital elevation model (earth elevation model) display of ground surface raster so that each point on the image has its corresponding height on the ground used as an effective tool in imaging the height and extracting data related to the height and elevation. Dem preparation is possible using a variety of information sources, including land surveying, aerial photography, radar, laser altimeters, and topographic maps. In this study, radar images are used to generate DEM and compared to provide an ideal model to be used in different basins (Krzystek, 1995; Ravinband et al., 2008). Digital elevation model from the ground can be obtained using airborne or spacecraft sensors. The space sensors can also offer digital model at different accuracy and wavelengths of the electromagnetic spectrum. Like Active sensors, they are single-channel and can only operate in a range of electromagnetic spectra called microwaves and do not have different bands as optical sensors (Krzystek, 1995). In general, the working method in active and inactive systems is different. Digital models obtained by optical sensors with high spatial resolution (at least 2.5 meters) can be used to make DSM (digital surface model). These sensors use visible waves to make a digital model, which means that the type of wave also changes. High resolution spatial sensors can give us images and DSMs with very high accuracy, which are not cost-effective due to high cost and low availability, and are mostly used in urban planning issues to provide a three-dimensional model of the city. But DEM can be obtained using radar images. The innovation of these models is the up-to-date of the available images and information that show the changes made on the ground. By producing DEMs from radar images, it has made the possibility to prepare topographic maps such as valleys, mountain peaks and desert areas, which require exorbitant costs. The research hypotheses are based on the fact that with a pair of radar images, a digital elevation model can be prepared with high accuracy. And with longer wavelengths, due to greater penetration, it is possible to provide high-precision DEM with an advantage that this model has over the topographic maps of the surveying organization. The purpose of DEM production, overall coverage area and the performance of many different domains which include high-precision waterway extraction in management issues, create dams, floods, etc (dam survey). It has been a better control on water flow due to precipitation, atmospheres and prevention of sediments and erosion of this model, digital to accelerate operations, engineering and construction projects, accurate, in road design, railway, transmission, water, electricity, gas, telephone, network design, hydrology, watershed, determining the areas sensitivity of the dam and to calculate the exact capacity of dam data.

2. Materials and Methods

Marvdasht is the city center of Fars province in Iran. This city is located 40 km north of Shiraz with mountainous and temperate climate. According to the census of 2016, the city population is 148,858 people. The geological configuration and structure of each region has a special impact on the development of that region, and this effect, in addition to creating settlements and related economic issues. The morphological and structural features of each geographical location, according to its climatic potential, draw the main lines of capabilities and locations.

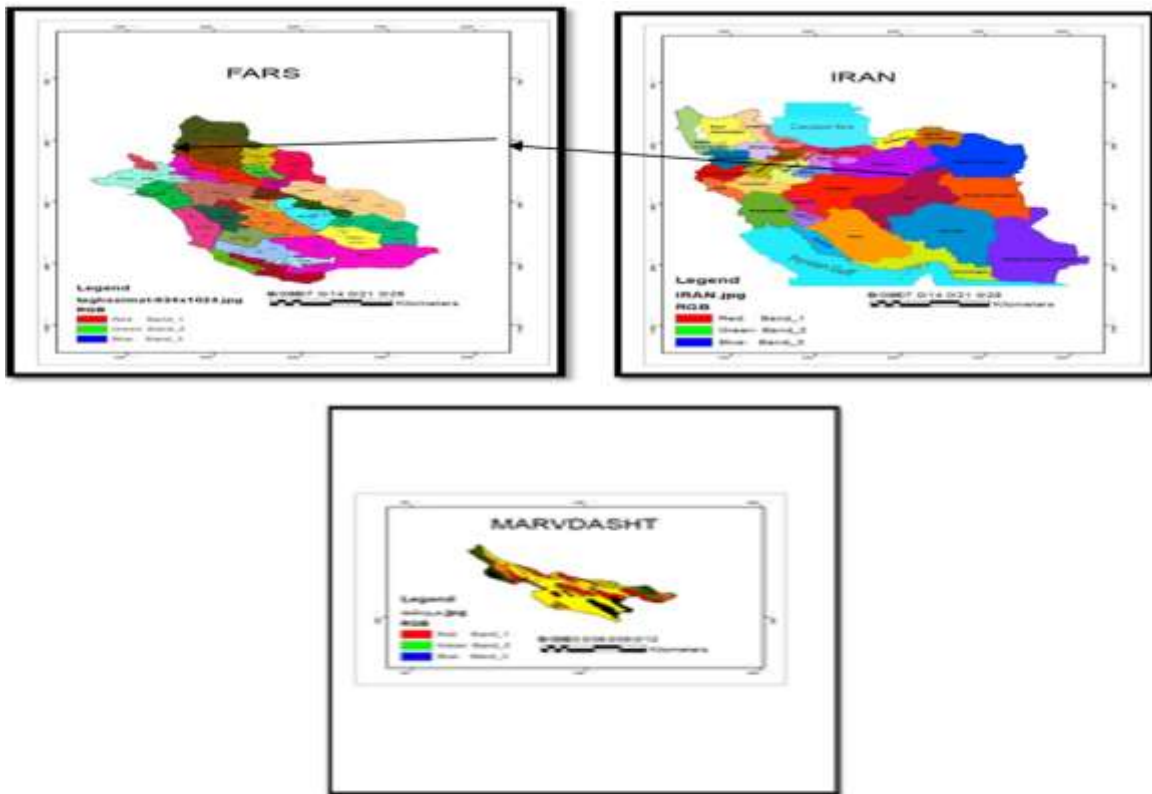


Figure 1. Marvdasht plain DEM study area map

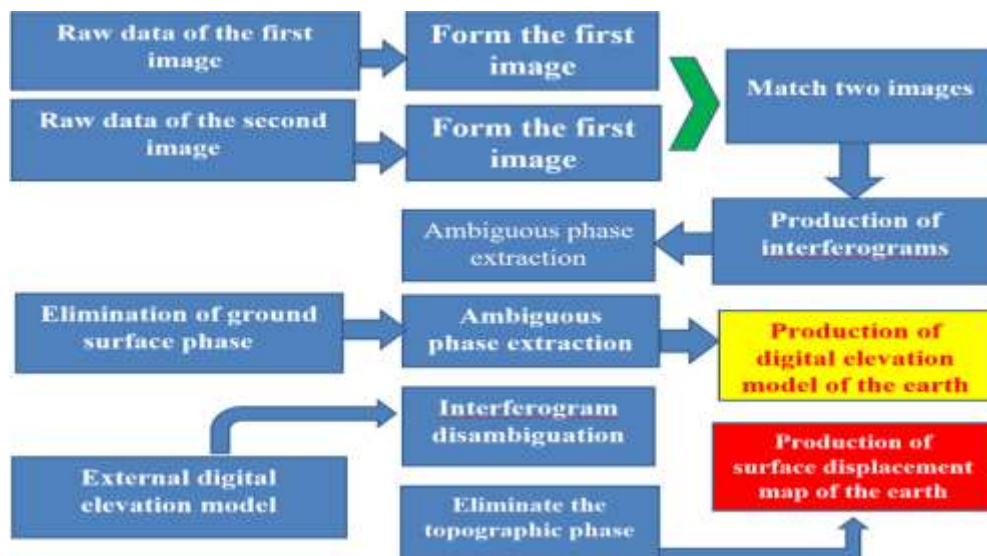


Figure 2. Steps to prepare a DEM map of C-band radar images for 2006-2007

3. Satellite Data used

In this study, we obtained radar images from the European Space Agency website and GPS data and data related to topographic maps and in person from their respective organizations. Using ASAR sensor images, the required information was collected from the study area. The ASAR sensor is one of the ENVISAT satellite sensors. The wavelength of the sensor is in the range of C band and is equal to 5.5 cm with a frequency of 5.331 GHz, which can record changes in the earth's surface up to an accuracy of less than a millimeter. Radar images from virtual aperture (SAR) radars with the ability to measure the length of the vector from the sensor to the ground, are widely used in measurements related to the preparation of digital elevation mapping (Fu and Li, 2019). Interferometry involves the gathering of precise elevation data using successive passes (or dual antenna reception) of spaceborne or airborne SAR. Subsequent images from nearly the same track are acquired and instead of examining the amplitude images, the phase information of the returned signals has been compared. The phase images are registered, and the differences in phase value for each pixel is measured, and displayed as an interferogram. A computation of "unwrapping" or integration phase, and geometric rectification are performed to determine altitude values. High accuracies have been achieved in demonstrations using both airborne (in the order of a few centimeters) and spaceborne data (in the order of 10m).

Table 1. Information for C-band radar images for 2006-2007 for DEM

Imaging mode	Image Mode	Wide Swath Mode	Altemating/Cross Polarization	Wave Mode	Global Monitoring
Polarization	VV or HH	VV or HH	HH/HV or VV/HH VV/VH or	VV or HH	VV or HH
Spatial resolution	28 m x 28 m	150 m x 150 m	29 m x 30 m	28 m x 30 m	950 m x 980 m
Extraction width	Up to 100 km	400 km	Up to 100 km	5km	>=400 km
Frequency	5.331 GHz (C-band)				

The Radar menu in SARscape software works with the power section and has nothing to do with phase. The Radar menu is not capable of working with the phase section and generating the Interferogram, therefore SARscape menu has been used for calculation. Before preparing the interferogram of the images, it is important to determine the base line between them so as to determine whether it is possible to perform the mentioned processing on these images or not? For which the baseline features of images are checked:

Table 2. Temporal and spatial baseline details of the ENVISAT ASAR sensor

Image history	Picture mode	Time interval	Spatial distance Normal Baseline	Elevation ambiguity	Range Shift (pixels)	Azimuth Shift (pixels)	Doppler effect difference between images
2006.06.27	ASAR-IMS	228-	346	80.808	12.507	55	3.3
2007.12.20	ASAR-IMS						

1. Base line estimation: To see how far apart the two images are and whether the distances between them allow us to construct an interferogram, we estimate the baseline. And then we make the interferogram. Image Interval: This means that the two ascending images were taken 33 days apart.

Normal Baseline: The distance between two imaging centers in two images. That is, the baseline of these two images is 364.23 meters. The best baseline for DEM production is between 300-400 meters.

Critical Baseline: The same as the maximum critical Baseline, which here is 2159 meters.

2 PI Ambiguity height: This means that the height ambiguity of these two images is equal to 49.9 meters, and the height accuracy of these two images is equal to a quarter of 2 PI Ambiguity height, which is equal to 6.52425.

Range Shift (pixels): The master image has a shift of 36.9 pixels in the range direction compared to the slave image.

Azimuth Shift (pixels): The master image has a shift of 17.3 pixels in the direction of Azimuth compared to the slave image.

Doppler Centroid diff: For all targets in these two images, if the value of Doppler Centroid diff is more than Critical Baseline, then it is not possible to interferogram two images.

Investigation of the Baseline properties of ASAR C-band detector images, which has been described above, the results are as follows. In this study, we used interferometry and time series analysis of interferograms to analyze ASAR sensor data and determine the amount of displacement.

A brief description to be mentioned:

Radar images from virtual aperture (SAR) radars with the ability to measure the length of the vector from the sensor to the ground, are widely used in measurements related to the preparation of digital elevation mapping (Fu and Li, 2019).

2. Generate interferogram and recognize all outputs and their characteristics

The phase difference between two SAR images is obtained by multiplying the first image by the conjugate of the second image:

$$y_1 = |y_1| \exp(i\varphi_1)$$

$$y_2 = |y_2| \exp(i\varphi_2)$$

$$I = y_1 y_2^* = |y_1| |y_2| \exp(j(\varphi_1 - \varphi_2)) \quad (1)$$

The image resulting from this mixed multiplication is called an interferogram. The amplitude of the interferogram is equal to the product of the amplitude of the two original images, and the phase of the interferogram is equal to the phase difference between the two images; therefore, interferogram pixels also have mixed values.

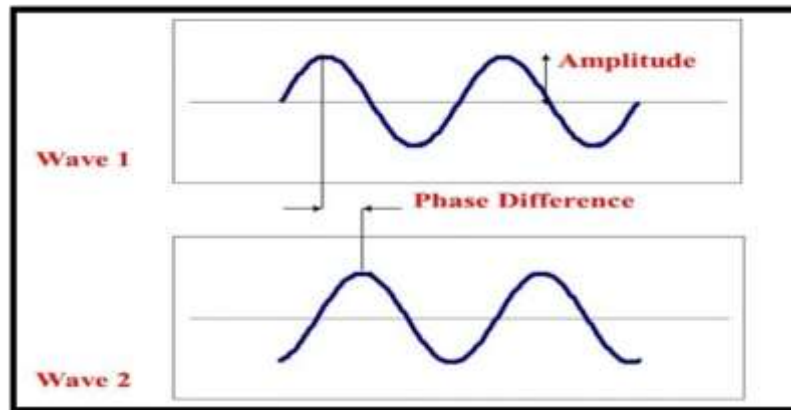


Figure 3. Phase difference between two images in interferogram production

Power image: The image from which the phase is separated and only gives us the Power output.

Int: It is the same interferogram, leading to the interferogram from which the topographic effect has not been removed

Dint: A file created in dint format from which the topographic effect has been removed, and if we want to calculate the amount of ground and fringes, we will use this file. In the output of the interferogram, three conditions may occur, which are: seen in the Interferogram, these phenomena are:

RAMP Phenomenon: This is a tape phenomenon, and occurs for two reasons: the effect of topography and the vibration of the sensor during imaging.

JAMP phenomenon: means phase jump. If there is a phase difference between two pixels of more than 10π , the JAMP phenomenon occurs

BAMP phenomenon: is the dome of the interferogram. If the interferogram becomes dome, it indicates a defect in the original data.

These three phenomena are not good phenomena. But the first two phenomena can be largely corrected with the help of filters.

Sint Image: This file is a Synthetic Interferogram, meaning a virtual interferogram made from a digital model. Srdem image: This is a digital model file created on an inclined arm.

Filter types and their function in radar images:

There are three types of filters so that we can produce the amount of coherence and also using filters to calculate the displacement of the fringes, each of these filters has advantages and disadvantages that are:

1. Adaptive filter: When filter without much coherence is used, the Adaptive filter does not touch the phases at all and maintains accuracy. Also, in the production stage, the digital elevation model has a great impact on elevation accuracy.

2. Goldstein filter: This filter strongly manipulates the phases in order to produce better fringes.

Performs interpolation in such a way as to bring all INCOHERENCIES closer together, that is, to coherent the waves as much as possible. So, it has to touch the phases and change them, so this filter reduces the accuracy of the work to some extent. We have to use this filter when our incoherency status is unfavorable.

3. Boxcar filter: This filter also does not touch the phases, so it is classified between Adaptive and Goldstein.

In this step, the amount of Incoherency is also calculated, which means that the amount of Incoherency varies between 0-1 per pixel. The closer it is to zero, the more incoherency the contents of the two pixels are in terms of phase. (Meaning that the waves are not coherent with each other on that pixel) and the closer they are to one, the more coherent the waves are. When coherent waves are returned to the satellite from all pixels, then it can give us very good fringes and then it can calculate the amount of displacement and the digital elevation model very accurately.

4. Correction and opening of phases through Phase unwrapping

In this step, it calculates the amount of displacement for all pixels, that is, it says where a few cm went up and where a few cm went down. Must convert all height changes to a factor of π . What this part does is break the whole topography and bring it between $-\pi$ to π . This is called phase opening, or Phase unwrapping

5. Reviewing the process of topographic effect and final modification of phases and satellite orbit through Refinement and Re-flattening: Refinement means again well done (improvement). At this stage, we want to once again check all the work that has happened from the beginning until now and make sure that there are no flaws in the work. It checks all the phases once again, it does two other things, one is to check the orbit once again. That is, it checks the distances of all the pixels on the earth from the original orbit (the orbit in which the satellite rotates) again, leaving no gaps or errors, and the actual elevation value is assigned.

6. Phase to Height stage: In this stage, it creates a turning topography and digital elevation model for us.

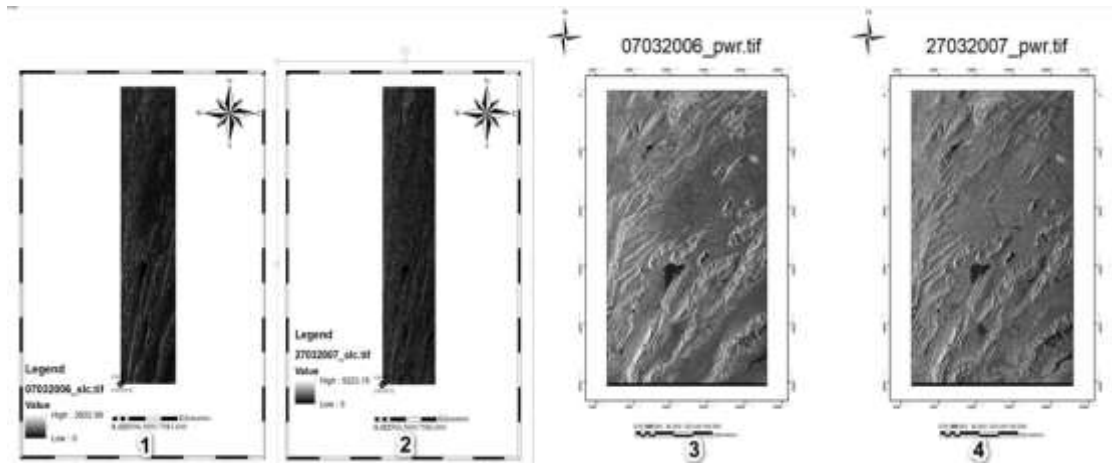


Figure 4.1. 2006 SLC image **Figure 4.2.** 2007 SLC image

Figure 4.3 & 4. Images from which the phase is separated and only gives us the Power output

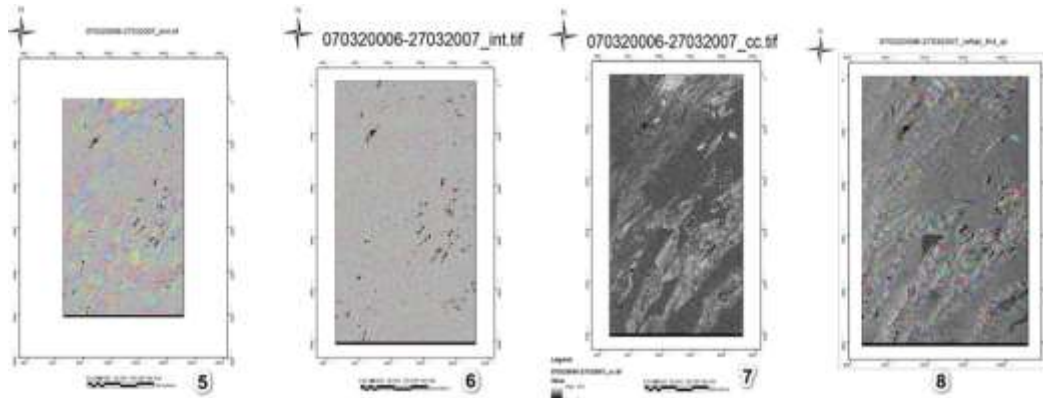


Figure 5.5. Topographic effect is removed and examined for fringe and displacement

Figure 5.6. Apply FILTER ADAPTER to INTERFEROGRAM.

Figure 5.7. Modified or REFELAT The ultimate product of DEM production

Figure 5.8. INCOHERENCE or areas without radar signal

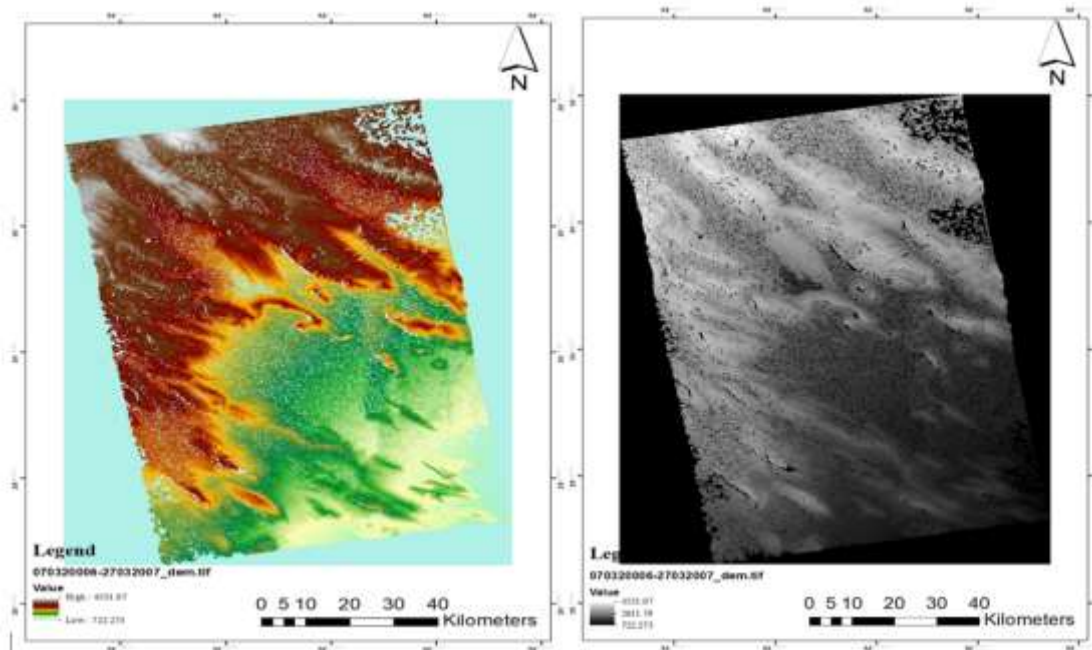


Figure 6. DEM map produced from ENVISATASAR band C radar images

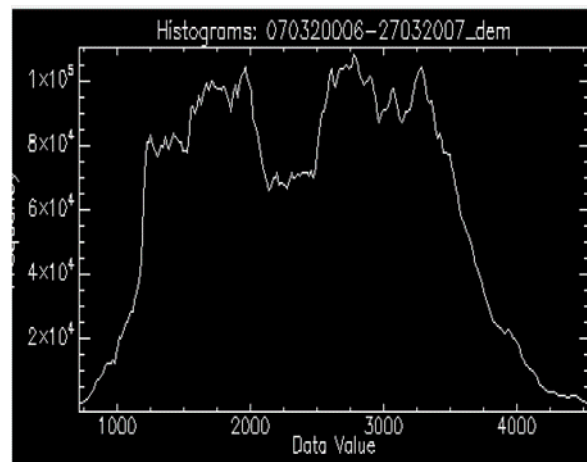


Figure 7. Histogram diagram of the digital elevation model of Marvdasht plain

Table 3. Comparison of height difference points obtained from C-band radar DEM 2006-2007 with GPS points

Station number	Point	Elevation	Eastervalu-radar	Height difference (meters)
1	Marvdasht Municipality Square	1600	1375.401	224.599
2	Shiraz-Marvdasht Petrochemical Complex	1595	1503.895	91.105
3	Green Mountain	1600	1572.826	27.174

4	Falunak	1606	1699.935	93.935
5	Thorn Company	1602	1660.128	55.128
6	Zarqanak	1605	1700.023	85.03
7	Goldsmiths	1615	1702.211	91.211
8	Razmanjan	1611	1786.325	166.325
9	Ismailabad	1618	1701.956	93.956
10	jeshnian	1618	1701.235	75.235
11	Ibrahimabad	1620	1846.233	237.233
12	Lower boulders	1608	2087.235	480.235
13	Kushk Hezar	1626	1698.023	85.023
14	Sheikh Abboud	1623	1551.325	52.673
15	Lapoe	1620	1352.327	241.673
16	Marvdasht Martyrs' Hill	1599	1433.26	165.74
17	Mansour Abad Airport	1611	1363.23	247.77
18	Innocent Abad	1601	1662.235	-61.235
19	High city three-way	1612	1630.757	-18.757
20	The peak of Eghlid Marvdasht road	1688	2212.486	524.486
21	Taleghani Town	1836	2823.599	987.599
22	Hot water	2177	2936.741	759.741
23	Pol Khan Mosque	2387	2730.331	343.331
24	Majabad	1603	2069.06	466.23
25	Maragloo	1605	1831.686	225.689
26	Low back	1608	2136.968	600.968
27	Darreh Abad	1596	1414.295	181.085
28	Town of Abarj	1597	1714.236	117.236
29	Marvdasht Municipality Square	1599	1714.412	115.412
30	Pilot point	1601	1595.175	5.825

Table 4. Comparison of height difference of topography points with GPS

Station number	Elevation	Rastervalu- topo	Elevation	Height difference (meters)
1	Marvdasht Municipality Square	1600	1601.795	1.795
2	Shiraz-Marvdasht Petrochemical Complex	1595	1695.865	100.865
3	Green Mountain	1600	1634.715	34.715
4	Falunak	1606	1613.233	7.231
5	Thorn Company	1602	1614.235	12.235
6	Zarqanak	1605	1567.231	37.769-
7	Goldsmiths	1615	1728.231	113.231
8	Razmanjan	1611	1710.231	99.231
9	Ismailabad	1618	1572.135	45.865-

10	jeshnian	1618		1577.157
11	Ibrahimabad	1620	1614.258	5.742-
12	Lower boulders	1608	1589.099	18.901-
13	Kushk Hezar	1626	1565.981	60.019
14	Sheikh Abboud	1623	1739.230	116.230
15	Lapoe	1620	1801.108	181.108
16	Marvdasht Martyrs' Hill	1599	1668.875	59.875
17	Mansour Abad Airport	1611	2033.246	426.426
18	Innocent Abad	1601	2013.542	393.542
19	High city three-way	1612	1601.103	11.897
20	The peak of Eghlid Marvdasht road	1688	1576.964	18.237
21	Taleghani Town	1836	1579.904	23.096
22	Hot water	2177	1557.714	47.286
23	Pol Khan Mosque	2387	1641.262	33.236-
24	Majabad	1603	1579.310	16.69
25	Maragloo	1605	1668.459	17.459-
26	Low back	1608	1621.459	22.459-
27	Darreh Abad	1596	1606.846	5.846-
28	Town of Abarj	1597	1730.231	77.231-
29	Marvdasht Municipality Square	1599	1727.257	79.257-
30	Pilot point	1601	1597.310	11.31-

Table 5. Comparison of difference in elevation of points obtained from C-band radar DEM with topography points

Station number	Point	Rastervalu-topo	Eastervalu-radar	Height difference (meters)
1	Marvdasht Municipality Square	1601.795	1375.401	226.358
2	Shiraz-Marvdasht Petrochemical Complex	1695.865	1503.895	191.970
3	Green Mountain	1634.715	1572.826	61.889
4	Falunak	1613.233	1699.935	86.702
5	Thorn Company	1567.231	1660.128	92.897
6	Zarqanak	1728.231	1700.023	28.208
7	Goldsmiths	1710.231	1702.211	8.020
8	Razmanjan	1614.258	1786.325	172.067
9	Ismailabad	1589.099	1701.956	112.085
10	jeshnian	1565.981	1701.235	135.254
11	Ibrahimabad	1668.875	1846.233	177.357
12	Lower boulders	2033.246	2087.235	53.989
13	Kushk Hezar	1601.103	1698.023	96.920
14	Sheikh Abboud	1576.964	1551.325	25.693
15	Lapoe	1547.702	1352.327	195.456

16	Marvdasht Martyrs' Hill	1600.055	1433.260	166.795
17	Mansour Abad Airport	1580.117	1662.235	82.118
18	Innocent Abad	1606.235	1630.757	24.522
19	High city three-way	2934.617	2936.741	2.124
20	The peak of Eghlid Marvdasht road	2683.379	2730.331	46.952
21	Taleghani Town	1557.714	1831.686	237.972
22	Hot water	1641.262	2136.968	495.706
23	Pol Khan Mosque	1579.310	1414.295	165.065
24	Majabad	1668.459	1714.236	45.777
25	Maragloo	1621.459	1714.412	92.953
26	Low back	1606.846	1595.175	11.652
27	Darreh Abad	1730.231	2912.900	1182.669
28	Town of Abarj	1727.257	2199.235	471.548
29	Marvdasht Municipality Square	1599	1714.412	115.412
30	Pilot point	1601	1597.310	11.31-

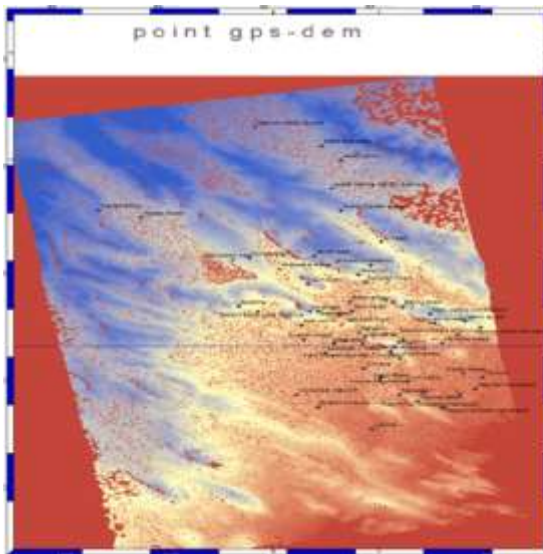


Figure 8. GPS capture points



Figure 9. Location map of GPS captured points

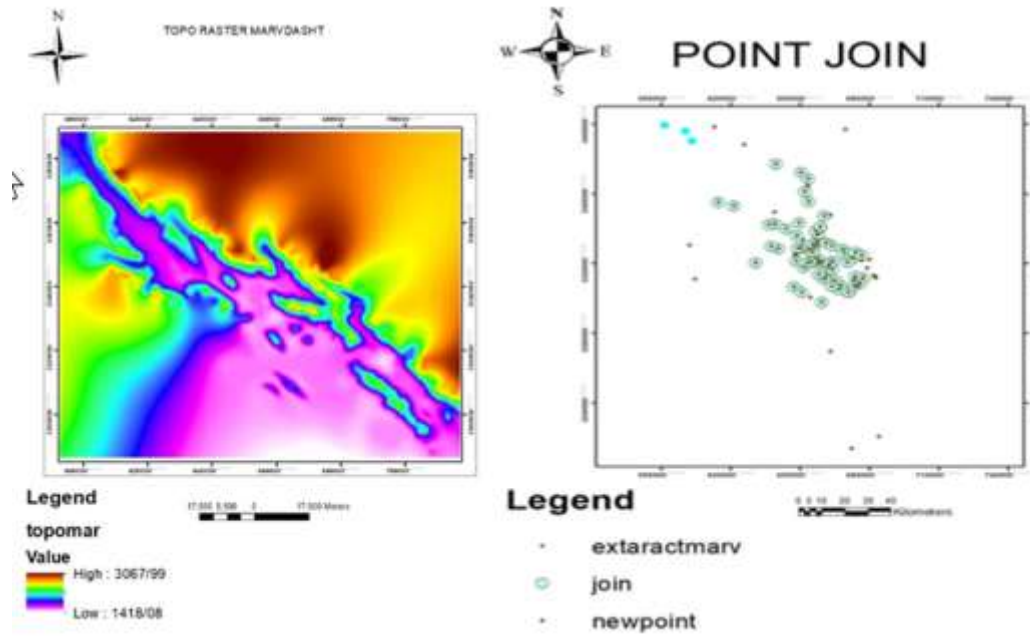


Figure 10. Topo Raster curve map and GPS interconnected points and topographic elevation points obtained from Marvdasht

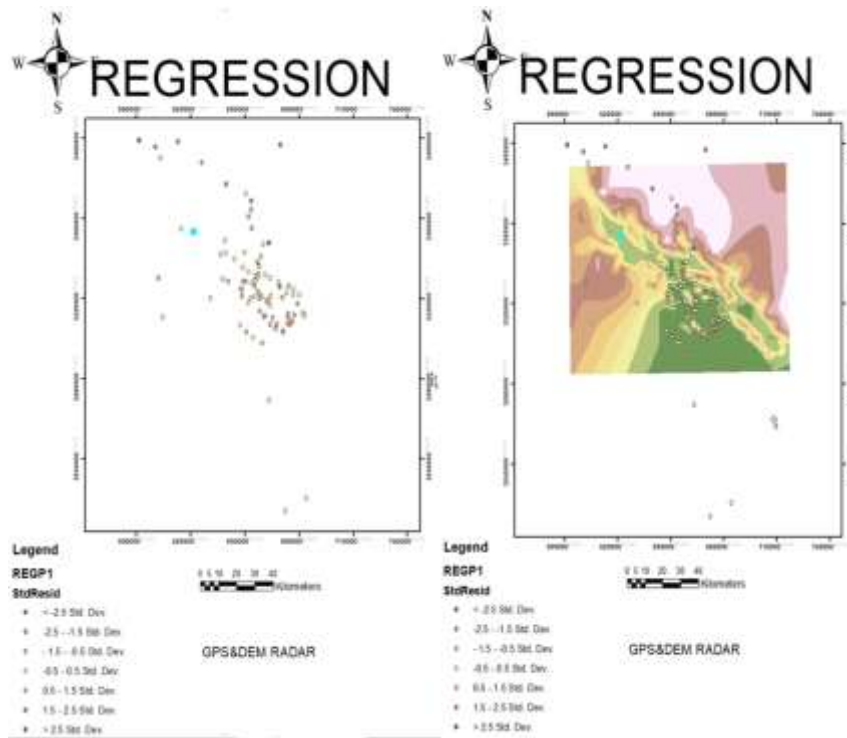


Figure 11. Weight regression map of GCP points, DEM and topography of Marvdasht

4. Results and Discussion

The results of radar image processing in the C bands of the Envi SAT ASAR sensor, comparing it with the data of the surveying organization, indicate that the data processed from the C band gives more favorable results and closer to the ground control points. However, due to the correlation between GCP and DEM points obtained from topography, the production conditions using satellite images are not favorable for the region. There are reasons to improve the correlation of topographic points. Radar images have Incoherency points, but due to the weight regression of points and less standard deviation of radar points compared to the topographic map of 1.25000 and GCP taken, the height points of radar images are in better and more favorable conditions. According to Table (Motahharinia et al. 2016), which shows the difference in criteria and this indicates the superiority of radar images for dem production, the digital model is produced and its comparison with topographic points shows the accuracy of satellite images in flat areas. In mountainous areas, due to the inclination angle of the points and the creation of INCOHERENCE points, it is not continuous as a shadow and the level curve lines are intermittent. Production of digital elevation model of the earth using radar images and comparing it with the reference digital elevation model whose elevation accuracy is one meter, the accuracy of the generated digital model was determined. The elevation of these points is compared with the height of the corresponding points on the digital elevation model produced. As expected, the results are more favorable in flat areas than in mountainous areas.

The results show that these satellite images have the capability of generating a relatively optimal DEM, particularly in non-mountainous area (Ghannadi, Enayati and Khesali, 2019). Considering the capability of these images and the technique of radar interferometry measurement in the production of digital elevation model of the earth and the existence of unique features of radar images, it is necessary to understand the importance of studying and using these images as much as possible in the production of digital elevation model (ghannadi et al., 2019). In this paper, three types of InSAR data with different wavelengths were used to generate and extract regional dem from the wetland. Each goldsten filter algorithm was used to eliminate phase noise. The control points were used from areas of the lagoon that had uniform coherence, and in order for the surface to be uniform, the second root was used to modify the circuits in a pixel. The result showed that the L band, PALAS ASAR, after validation is suitable for DEM production (Amighpai, Arabi, and Talebi, 2009). However, the DEM from the SENTINEL-1A C-band satellite and the TERRASAR X-band satellite are less coherent due to the shorter wavelength, and the DEM does not produce accurate results. DEM made of INSAR images has higher quality and accuracy than topographic maps (Ghannadi, Enayati and Khesali, 2019). Methods of data acquisition; nature of input data, vertical resolution and techniques employed to develop DEM are basic requirements where the DEM quality depends on and the good accuracy of DEM can be achieved by increasing the number of GCP by San and Suzen (2005) (Fu and Li, 2019). This paper has showed the results of experiment of application the InSAR technique for DEM generation. It is gaining importance due to data availability for all weather and day and night. More over since phase information is used to derive topography, it is possible to detect centi meter level changes in topography using differential interferometry (Ghannadi, Enayati and Khesali, 2019). According to the above results and the comparison between traditional techniques and modern (images, satellite and radar) can be the result of the expression. The technologies of the recent more suitable than the traditional can be, though with improved images InSAR can be DEM high production. GPS points are not affordable at a wide level, and a DEM with their quality and accuracy is low and above 20 meters. The process of generating DEM from satellite images and radar with precision quality and high precision, high as well as high speed production and low cost of priority, but the fundamental problem of images, radar wavelength, they are in mountainous areas and areas of vegetation is high. The overall result of radar and satellite imagery is the advantage and superiority over other traditional methods and topography can be extracted in centimeters.

5. Acknowledgements

Greetings and best regards to Dr. Al-Modarresi, the honorable professor that in all stages of the dissertation as well as the article, with patience, guiding and helping me and also thanking the honorable professor Dr. Jamali and all those who have participated in the organization of this conference.

References

- Amighpai, M., Arabi, S., & Talebi, A. (2009). Investigation of Yazd subsidence using radar interferometry and accurate leveling. *National Geomatics Conference*.
- Fu, B., & Li, Y. (2019). Study on accuracy assessment of DEM in the marsh using with interferometric PALSAR, Sentinel-1A and TerraSAR-X images. *The International Archives of the Photogrammetry, Remote Sensing and Spatial Information Sciences*, Volume XLII-3/W10, 2020 International Conference on Geomatics in the Big Data Era (ICGBD), Guilin, Guangxi, China.
- Gabriel, A. K., & Goldstein, R. M. (1988). Crossed orbit interferometry: theory and experimental results from SIR-C. *International Journal of Remote Sensing*, 9(5), 857–872.
- Ghannadi, M. A., Enayati, H., & Khesali, E. (2019). Generating Digital Elevation Model of the Earth Using Sentinel-1 Images and Interferometry. *Geographical data*, 27(108),109-121. Retrieved from: <https://www.sid.ir/en/journal/ViewPaper.aspx?id=665105>
https://www.researchgate.net/publication/209805236_Digital_elevation_model_DEM_generation_and_accuracy_assessment_from_ASTER_stereo_data
- Krzystek, P. (1995). New investigations into the practical performance of automatic DEM generation. *Proceedings, ACSM /ASPRS annual convention charlotte, North Carolina, American Society for photogrammetry and remote sensing*. 20, 448-500.
- Le Toan, T., Quegan, S., Davidson, M.W.J., Balzter, H., Paillou, P., Papathanassiou, K., Plummer, S., Rocca, F., Saatchi, S., & Shugart, H. (2011). The BIOMASS mission: Mapping global forest biomass to better understand the terrestrial carbon cycle. *Remote Sensing Environment*, 115, 2850–2860.
- Motahharinia, A. A., Al-Modarresi, S. A., & Naqdi, K. (2016). *Production and comparison of digital model of DEM altitude) using radar differential interferometry technique in C and X band waves*.
- Pakdaman, M. S., Al-Modarresi, S. A., & Sarkar Gardakani, A. (2014). Detection of subsidence dimensions of Imam Khomeini Airport using radar interferometry method. *The first conference on spatial sciences in land management*.
- Ravinband, M. V., & Jain, K. (2008). Digital Elevation Model accuracy aspects (version 8.31.06) *Journal of applied sciences*, 8(1), 134- 139.
- Vivek Kumar Singh, P. K., Champati, R., & Jeyaseelan, A. T. Jharkhand Space Applications Center, Ranchi, Dept. of Information Technology, Government of Jharkhand, India.
- ghannadi, M. A., Enayati, H., & Khesali, E. (2019). Generating Digital Elevation Model of the Earth Using Sentinel-1 Images and Interferometry, *Quarterly Journal of Geographical Information*, 27(108).